Additional material

- ✓ Thirumalai - Mountain metric
- ✓ Traveling Density Wave model
- ✓ Slider block models

not at present:

- Klein - Unger
- Boltzmann distn - Rundle stuff
  Egolf stuff

Nucleation

Notes by W. Klein — main reference

We begin by considering phenomenology, discussing the basic physical processes

Data we use is both numerical & real

Let us begin with a common model, the Van der Waals eqn of state

1-component fluid

$$\left(P + \frac{a}{V^2}\right)(V-b) = RT \qquad \text{——— (*)}$$

V = vol. per mol or specific volume

a & b are phenomenological parameters.

Here b is the "excluded volume" term and a is the "molecular attraction" term.

We can actually reduce (*) to a simpler form by defining the 3 parameter

$$P_c = \frac{a}{27b^2} \; ; \quad T_c = \frac{8a}{27Rb} \; ;$$

$$V_c = 3b$$

Using the new variables:

$$\tilde{P} = \frac{P}{P_c} \; ; \quad \tilde{V} = \frac{V}{V_c} \; ; \quad \tilde{T} = \frac{T}{T_c}$$

$$\Rightarrow \left(\tilde{P} + \frac{3}{\tilde{V}^2}\right)\left(3\tilde{V} - 1\right) = 8\tilde{T}$$

A Plot of the VdW equation looks like this:

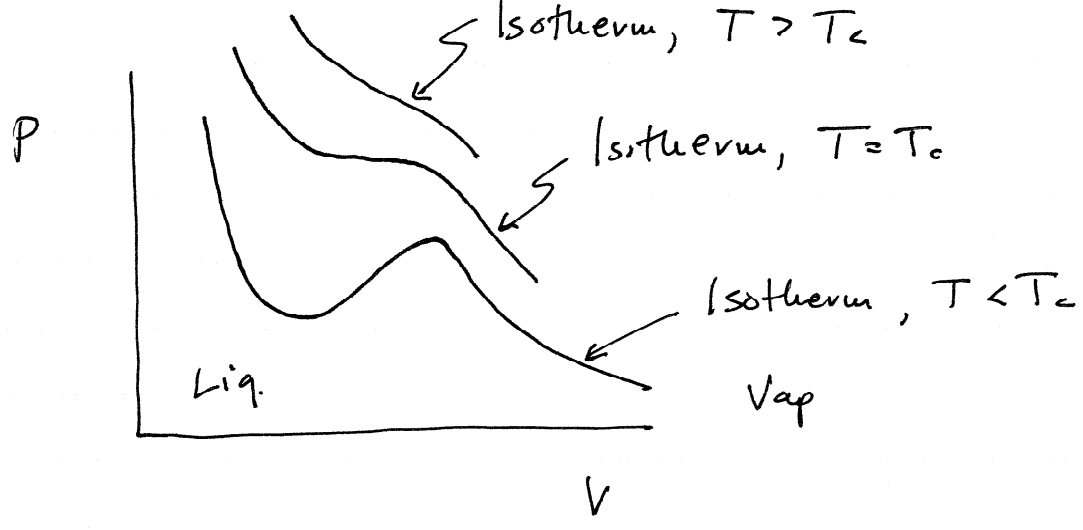

If we plot on P–ρ axes, then the regions are reversed

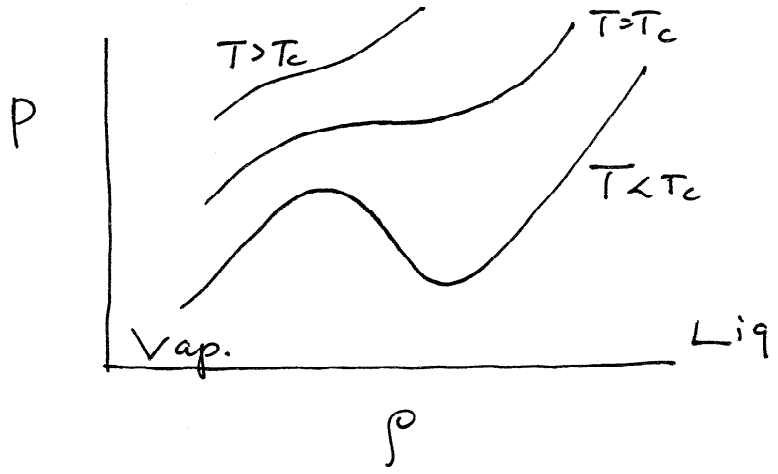

For $T<T_c$, consider the curve:

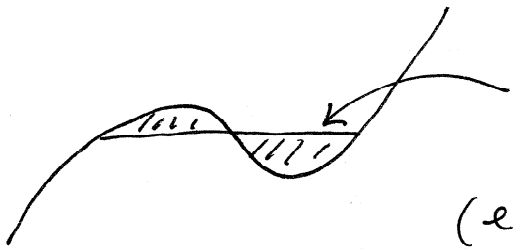

Moreover, for $T<T_c$, there is the question of stability of the system w.r.t. phase transitions:

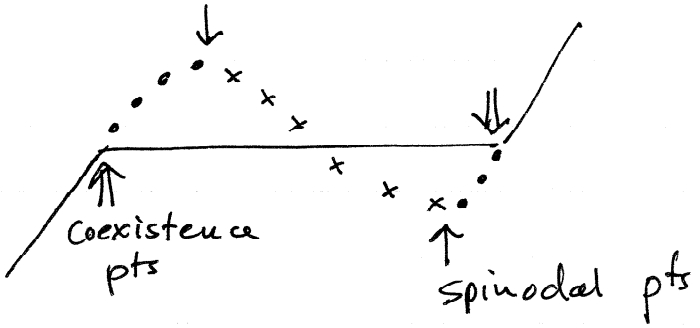

——— = stable phase — equilibrium
• • • • = metastable phase — nonequilibrium
× × × × = unstable — nonequilibrium

In this course we are interested in the parts of the curve corresponding to the dots & the crosses.

Magnetic Systems : As we will see, magnetic (spin) systems have a very similar phenomenology. Stable, metastable, and unstable regions can be defined on the M - h-T phase diagram

On the unstable part of the curve, the isothermal compressibility

$$\kappa_T \sim \left| \frac{\partial \rho}{\partial p} \Big|_T \right|^{-1} < 0$$

which implies that increasing the pressure lowers the density ρ

This silly result is due to the idea that we are trying to describe a

non-equilibrium process with an equilibrium theory.

In figure: dotted lines represent metastable states.

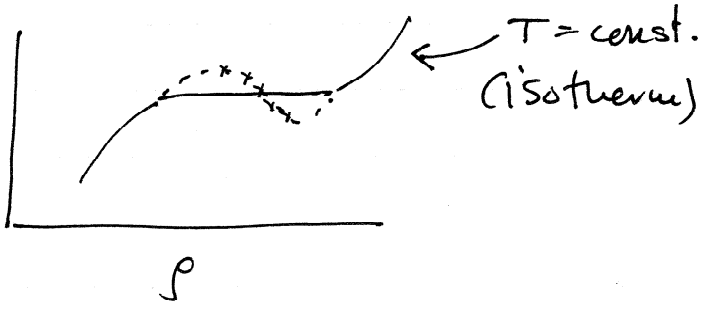

Another way of representing this curve is by remembering the Gibbs-Duhem relation:

$$d\mu = v\,dp - s\,dT$$

μ: Gibbs free energy per unit mass. { chemical potential

v: specific volume

s: specific entropy

Along an isotherm, $dT = 0$

$$\Longrightarrow \quad \mu(P,T) = \int_{P_i}^{P} v\,dP' + C(T)$$

(see Harvey S. Robertson, "Statistical Thermophysics" Prentice Hall, 1998)

We obtain:

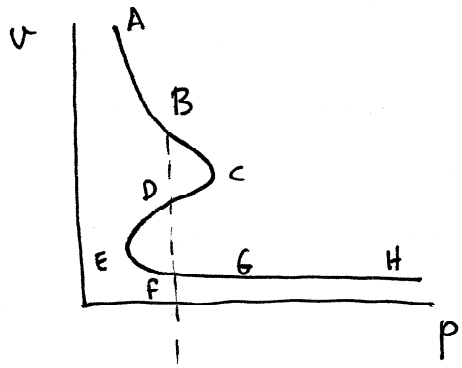

P-v diagram turned on side

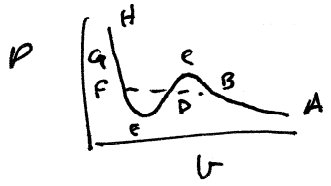

Use Van der Waals

$$\left(P + \frac{an^2}{V^2}\right)(V - nb) = nRT$$

moles

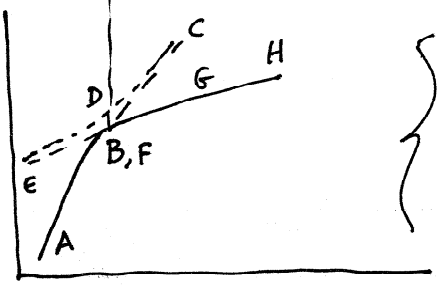

A-B,F-G H is convex, indicating Thermodyn. stability.

E-D-C is concave indicating thermodyn. instability.

Notice that solid lines on μ-P diagram have lowest free energy for that value of P & are thus the stable phase

So metastable state is a state of local stability, not global stability

We can also plot the loci of the coexistence pts and spinodal pts:

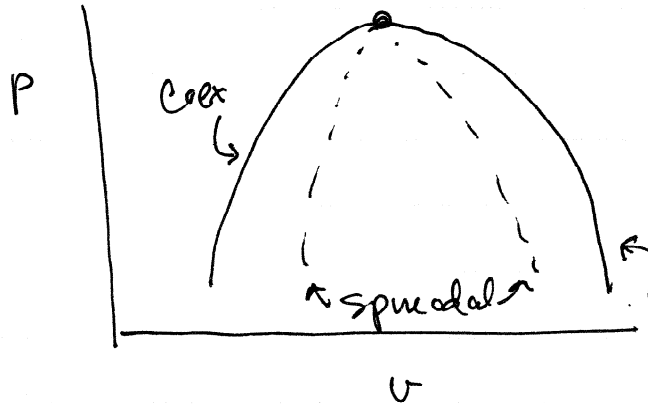

using the isotherms

and (etc.)

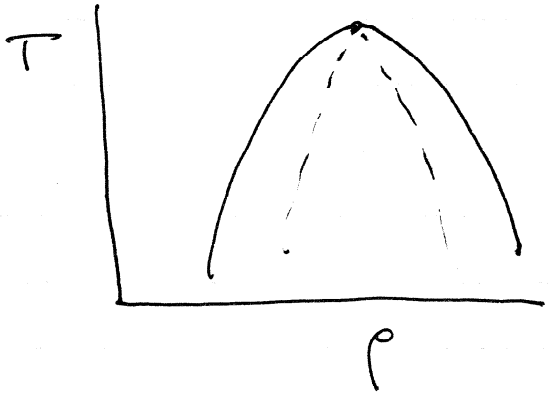

using the isobars (const. pressure lines)

Neither unstable or metastable states are global minima, so they must decay, to lower energy states.

Definition: "Order parameter"

Order parameter is the variable that specifies the structure of the phase Transition. It changes from one value to another at the phase transition.

e.g. liq → gas, $\Delta S \gtrless 0$

- If O.P. is discontinuous at phase transition, ⇒ first order

C $\gtrless 0$ or cusp.

- If derivative of O.P. is discontinuous at phase transition, then ⇒ 2nd order. with critical pts, scaling, etc.

Ex: Nucleation & growth of density variations in an Iron-Aluminum (Fe-Al.) alloy undergoing phase separation

1) Columns represent temporal evolution (top to bottom)
2) 1st & last columns: Evolution

subsequent to a quench to different pts in the metastable region.

3) Middle column is result of a quench into an unstable state.

Quench to metastable states show the birth & growth of droplets.

Quench to unstable state shows spinodal decomposition & subsequent domain coarsening

Remarks: Note that even after 10,000 minutes, system is nowhere close to an equilibrium state.

Also, study of time evolution ("kinetics" or "dynamics") involves study of random interfaces, & topological singularities.

KL-9A

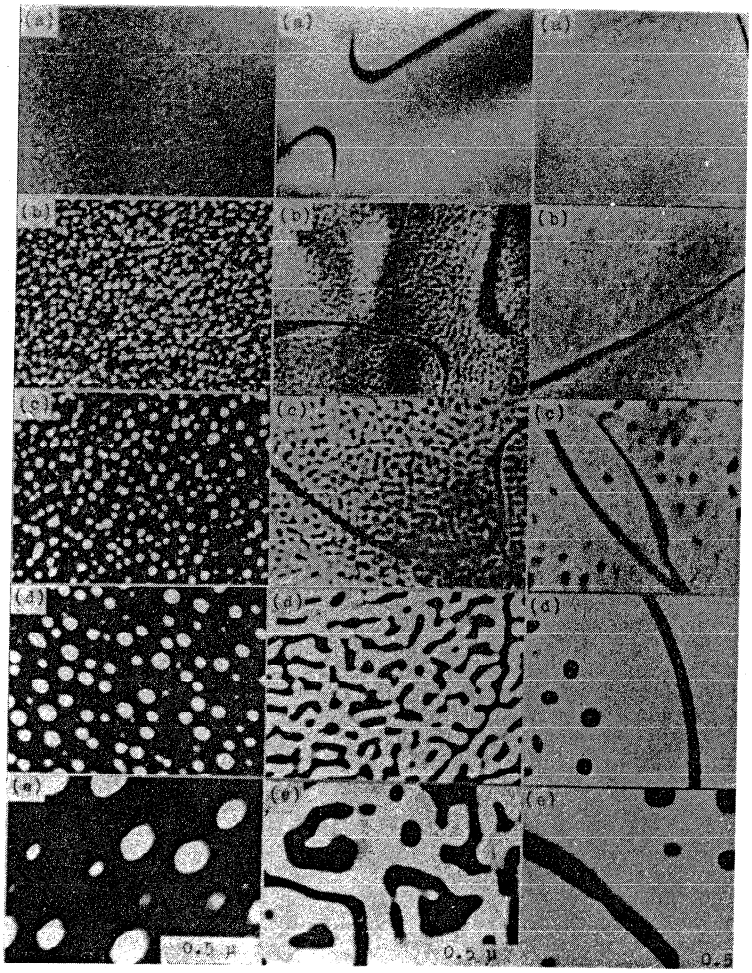

Figure 1.3 : Domain structures imaged with B_2 superlattice reflection in 23.0, 24.7 and 24.9 at. % Al alloys, from left to right. The samples are quenched from 630°C and annealed at 570°C in the case of 23.0 and 24.7 at. % Al alloys and at. 568°C in the case of 24.9 at. % Al alloy.
a) as quenched; b) annealed for 15 min. in 23.0 and 24.9 at. % Al and for 10 min. in 24.7 at. % Al alloy; c) 100 min.; d) 1000 min.; e) 10000 min..
(From Oki, Sagana and Eguchi, Ref. [4].)

of bulk two pha
that well defin
tion of metasta
interfaces. Ind
namics of metas
the general pro
examples includ
ly, if one exam
there is a self
tion of the pha
the bottom phot
that each of th
immediately abo
tion is invaria
scaling. These
eral chapters o

It is also
tering experime
particular syst
a glass is show

Figure 1.4 : Pl
th
sy
(F

From JD Gunton & M Droz,
"Intro. to Theory of Metastable &
Unstable States", Springer Lecture
notes, 183, 1983.

DEFINITIONS — TERMINOLOGY

Finally, we note the following.

1) Nucleation is mechanism by which meta stable state decays ⇒ formation & growth of droplets (bubbles) > late stage growth

2) Spinodal Decomposition is the mechanism by which unstable state decays (order parameter conserved)

3) Continuous Ordering' is decay from unstable state (if order parameter not conserved).

⇒ We now construct simple theories to describe these three processes.

Begin with simple theory of Nucleation

Nucleation - Simple Theory

We have treated metastability within the context of an equilibrium Theory. We will see that there is no contradiction in general, but we now develop a better foundation for this.

Ising Model: Spins $S_i = \pm 1$
Applied field h
Interaction K_{ij}

$$(*) \qquad H_I = -\sum_{ij} K_{ij} S_i S_j - h \sum_i S_i$$

Klein's notes: $-\beta H = \sum_{ij} K_{ij} S_i S_j - h \sum_i S_i$

We will adopt notation for this course that is consistent with Klein's notes.
Thus we will assume (*) as our form ("standard") → also $K_{ij} > 0 \ \forall i,j$

→ until further notice

Ising Model

Binary Model.

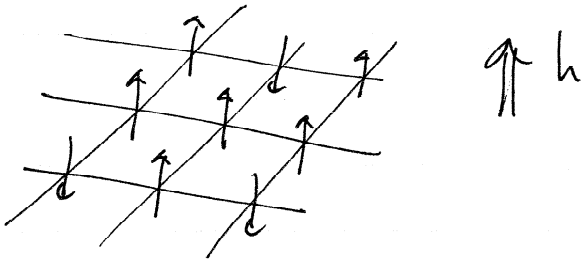

Ising model can also be used as a model for a "lattice gas". i.e.,

$$\rho_i = \frac{(1+S_i)}{2}, \quad \in (0,1)$$

Schematic plot of magnetization m as a function of h for $T < T_c$:

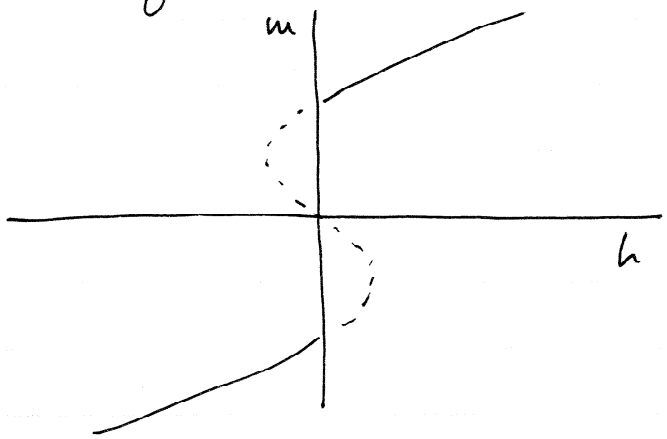

meanfield version of model

Lattice gas: $\rho = \frac{(1+m)}{2}$

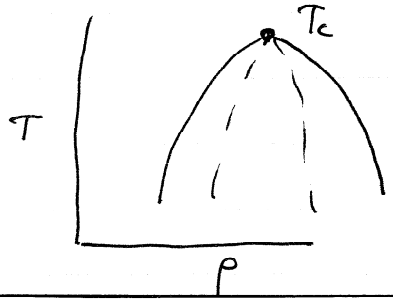

Coarse-grained free energy:

Define a local coarse-grained order parameter $\psi(\vec{x})$

$$\psi(\vec{x}) = \frac{1}{L^d} \sum_{i \in L(\vec{x})} s_i$$

$L(\vec{x})$ is a box of size L centered at $\vec{x}$ in d-dimensions.

Typically, $L >> a$, where a is atomic (lattice) scale. Also $L << \ell$, where ℓ is the dominant statistical length in system (e.g., ℓ = size of system; or ℓ = droplet size, etc.)

So physics is not washed out by coarse-graining procedure

ℓ need not be correlation length !

We postulate a phenomenological free energy $F(\psi)$

Mixing Entropy

$S = k \log W \quad W = \frac{N!}{n_1!(N-n_1)!}$

$\rightarrow k\left(\frac{N_+}{N}\log\frac{N_+}{N} + \frac{N_-}{N}\log\frac{N_-}{N}\right)$

$$F(\psi) = -h\int \psi(\vec{x})\,d\vec{x} - \frac{1}{2}\iint K(|\vec{x}-\vec{y}|)\,\psi(\vec{x})\,\psi(\vec{y})\,d\vec{x}\,d\vec{y}$$

$$- k_B T \int (1+\psi(\vec{x}))\log(1+\psi(\vec{x}))\,d\vec{x}$$

$$- k_B T \int (1-\psi(\vec{x}))\log(1-\psi(\vec{x}))\,d\vec{x}$$

ψ is a fluctuation ($\frac{N_+}{N} = 1+\psi$)

Note: 1st term is interaction with external field of spins in a coarse-grained block

2nd term is interaction between coarse-grained blocks

3rd & 4th terms are entropy of mixing $\frac{\text{avg}}{\text{1}}$ spins in coarse-grained block.

Further simplification:

1) Assume $\psi(\vec{x})$ is small so logs can be expanded

2) "Gradient expansion" —

Going to Fourier space & using Parseval's theorem —

$$\frac{1}{2}\iint K(|\vec{x}-\vec{y}|)\,\psi(\vec{x})\,\psi(\vec{y})\,d\vec{x}\,d\vec{y}$$

use $\psi(\vec{x}) = \frac{1}{\sqrt{2\pi}}\int_{-\infty}^{\infty}\hat{\psi}(\vec{k})\,e^{i\vec{k}\cdot\vec{x}}\,dk$ etc.

$$= \frac{1}{2}\int\int \hat{K}(|k|)\,\hat{\psi}(\vec{k})\,\hat{\psi}(-\vec{k})\,d\vec{k}$$

Expanding $\hat{K}(|k|) \approx 2\hat{K}(0) + 2R^2 \overset{\nabla^2}{\downarrow} k^2 + \cdots$

$$= \hat{K}(0)\int(\psi(\vec{x}))^2 d\vec{x} + R^2\int(\nabla\psi(\vec{x}))^2 d\vec{x} + \cdots$$

where $R^2 = \int x^2 K(x)\,dx$, $x = |\vec{x}|$,
and we have integrated by parts.

Truncation of k-series for K is justified by assumption that only long-wavelength properties govern the phase transition.

So our model becomes:

$$F(\psi) = \int d\vec{x}\,\{R^2(\nabla\psi(\vec{x}))^2 + \epsilon\psi^2(\vec{x}) + \psi^4(\vec{x}) - h\,\psi(\vec{x})\}$$

where $\epsilon = k_B T - \hat{K}(0)$

This is the Ginzburg-Landau free energy, which can be obtained by other means as well ("Hubbard-Stratonovich", or "Gaussian" transform).

Also called the Ginzburg-Landau-Wilson Hamiltonian.

Aside: This is clearly a near-mean-field model, since we have explicitly assumed that only long-wavelength fluctuations matter. So we should expect G-L-W free energy should produce results, such as scaling exponents, that are (near) meanfield as well.

If we assume no fluctuations, ("thermodyn. limit"), then we find meanfield:

$$f(\psi) = \frac{F(\psi)}{V} = \epsilon\psi^2 + \psi^4 - h\psi$$

where V is volume of the system.

From $\epsilon = k_B T - \hat{K}(0)$ $\quad (\hat{K}(0) > 0)$

it is clear that as $T \to \infty$, (i.e., high T)

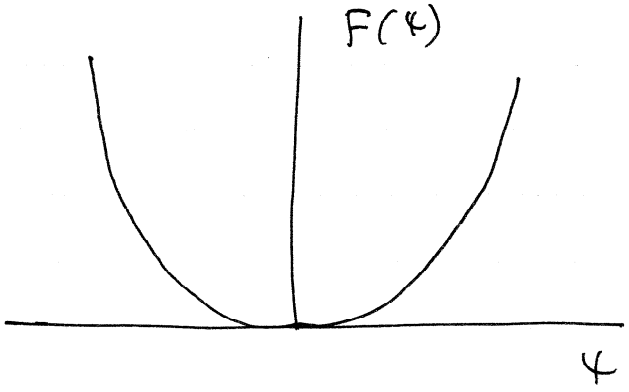

$\epsilon > 0$

one minimum

As T is lowered below critical temp $T_c = \frac{\hat{K}(0)}{k_B}$ we have:

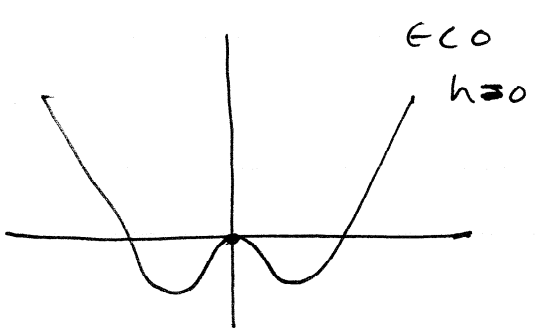

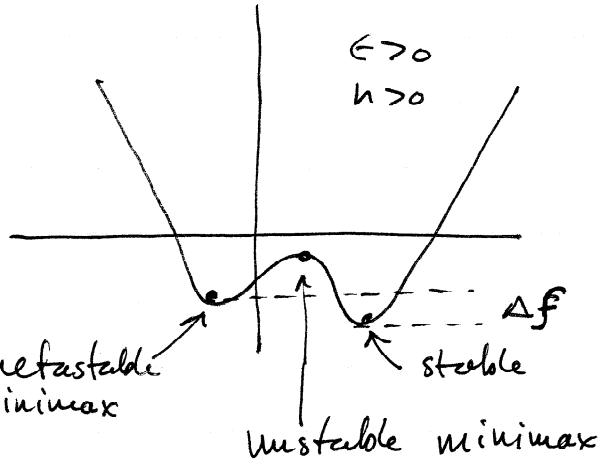

As we change h, the metastable, unstable, and stable points trace out

the branches shown by the $\mu(P)$ vs p curve for a van der Waals liquid.

Metastable state acts like a stable state until a thermodyn. fluctuation "probes" thermodyn. state space far enough so that system "discovers" there is a lower minimum.

Assumption: Fluctuations that initiate decay of the metastable state can be treated as equil. fluctuations about the metastable local minimum of the free energy. Holds if metastable lifetime is long enough so that metastable equil. is attained. (No one knows how long this is)

Experimentally - Metastable state can be very long-lived

Classical Theory of Nucleation - Assumptions:

1. Nucleation initiated by isolated, non-interacting droplets that are treated as fluctuations about metastable minimum

2. Droplets are compact, surface & interior can be considered separately

3. Interior & surface free energies are well defined

4. Surface free energy density (surface tension) is insensitive to quench depth

5. Interior free energy density is equal to free energy density of stable phase

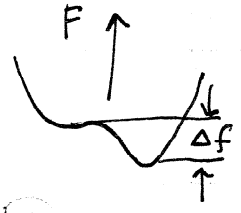

$$\Delta F = -|\Delta f| r^d + \sigma r^{d-1}$$

(d ← dimension of space)

- $|\Delta f|$: bulk f.e. density — difference between metastable state & droplet interior
- σ: surface tension (surface f.e.) density

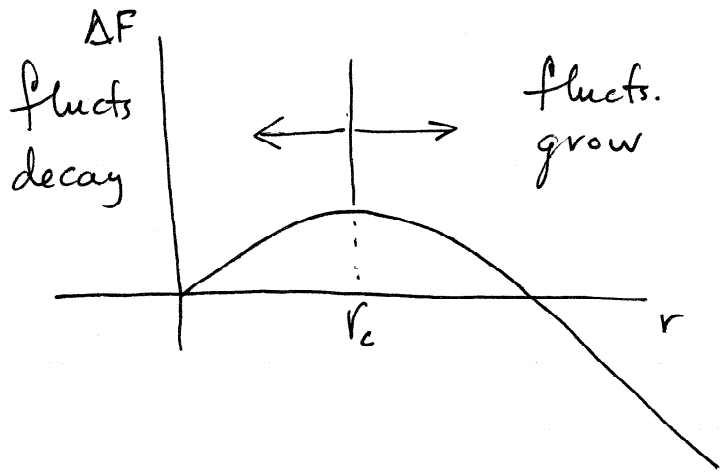

$$\frac{d\,\Delta F}{dr} = 0 \Rightarrow r_c = \frac{\sigma}{|\Delta f|}\left(\frac{d-1}{d}\right)$$

$$\Rightarrow \Delta F = \left(\frac{d-1}{d}\right)^{d-1}\left(\frac{2d-1}{d}\right)\frac{\sigma^d}{\Delta f^{d-1}}$$

Droplets are assumed <u>non-interacting</u>, so probability of finding a droplet (critical) is inversely proportional to time spent in metastable state, before one appears.

Thus,

$$\tau \propto \exp\left(\frac{\Delta F}{k_B T}\right)$$

If quench into metastable state terminates near coexistence curve, $\Delta f << 1$ and $\tau \to \infty$.

We assumed system would be in metastable equilibrium before critical droplet ($r = r_c$) appeared. For large τ (shallow quench) this is reasonable.

But, for a deep quench, $\Delta f \sim$ few $k_B T$, and τ can become small. Assumption of metastable equilibrium is then violated. Quench depth at which this takes place is often called <u>limit of metastability</u>, or sometimes the "Becker-Doring" limit:

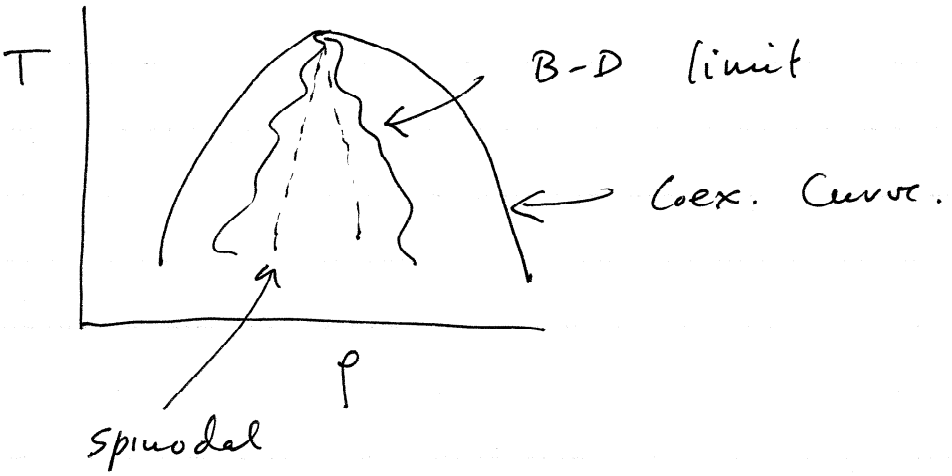

<u>Note</u>: Analysis that led to classical theory of nucleation is not mean-field

1. We have assumed critical droplets are non-interacting.

2. Quench depth $\Delta f \propto h$ so that

$$\frac{1}{\Delta f^{d-1}} \sim \frac{1}{h^2} \quad \text{in } d=3.$$

3. τ^{-1} is nucleation rate, or number of critical droplets per unit volume per unit time

Following figure is from Heermann et al (1984)

→ a simulation of an Ising model (nearest neighbor, non mean-field)

Fit to a straight line is pretty good.

KL -21A

J. Stat. Phys 36, 447 (1984)

droplets overcoming the nucleation barrier, and determined from n_s^* for the temperature $T/T_c = 0.59$, is shown in Fig. 6. The straight line is the prediction from Eq. (3.2.1) where the classical prefactor was used and the surface tension was taken to be $=3.1$ (cf. Table 1). For small nucleation rates (small applied field) the data, however, indicate some curvature and are probably not just statistical fluctuations or finite size effects. Kehr and Binder[24] interpreted these deviations as being due to the transition from spherical to cubical droplet shape when the droplet size increases due to a decreasing field.

Deviation from the expected behavior of the nucleation rate was also found for the temperature $T/T_c = 0.86$ (cf. Fig. 7). The nucleation rate shows a curvature and not the expected linear behavior.

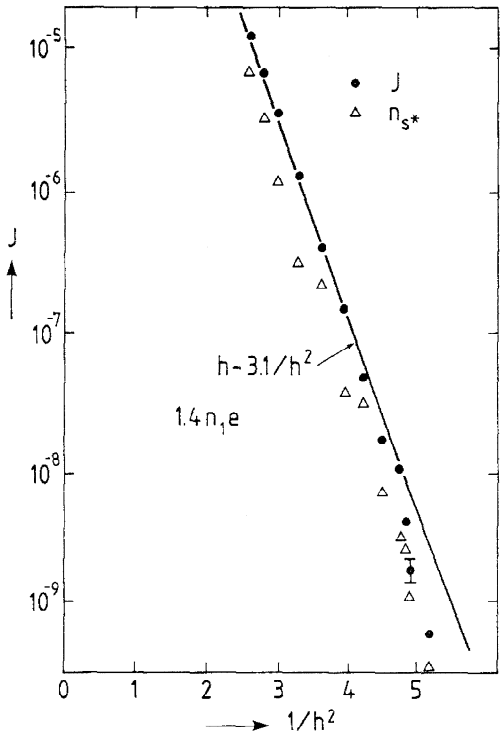

Fig. 6. Nucleation rate plotted logarithmically versus $1/h^2$ for the temperature $T/T_c = 0.59$. The solid line is the prediction from the classical nucleation theory with the surface tension $\sigma/k_B T$ taken from series expansions (Ref. 22). The crosses give the number n_s^* of critical nuclei, as found by our simulations. The dots give the observed nucleation rate.

Continuous Ordering

Quench into unstable region —
equilibrium ideas no longer work.

Consider laws governing dynamical evolution.

H-H Model A

a) Order parameter not conserved — all extensive variables allowed to fluctuate

H-H model B

b) Order parameter conserved

Taxonomy proposed by Hohenberg-Halperin, Rev. Mod. Phys., 49, 435 (1977).

Model A: $\int \psi(x,t)\, d\vec{x} = \rho(t)$ density

Thermodynamics

$$\frac{\partial \rho}{\partial t} = -M \mu(t)$$

M ← mobility

$\mu(t)$ ← chemical potential.

Also $\mu(t) = \dfrac{\partial F(\rho)}{\partial \rho(t)}$

So for coarse-grained model,

$$\frac{\partial \psi(\vec{x},t)}{\partial t} = -M\mu(\vec{x},t)$$

$$= -M \frac{\delta F[\psi(\vec{x},t)]}{\delta \psi(\vec{x},t)} \rangle \text{ F.D.}$$

The functional derivative is defined as:

If $F = F[\psi(\vec{x},t)]$ then

Goldenfeld pg 157 $\langle$

$$\frac{\delta F[\psi(\vec{x},t)]}{\delta \psi(\vec{x},t)} \equiv \lim_{\epsilon \to 0} \frac{F[\psi(\vec{x},t) + \epsilon \delta(\vec{x}-\vec{x}')] - F[\psi(\vec{x},t)]}{\epsilon}$$

This relation has the following properties:

$$\frac{\delta}{\delta \eta(\vec{r})} \int d\vec{r}\, \eta(\vec{r}') = 1$$

$$\frac{\delta}{\delta \eta(\vec{r})} \eta(\vec{r}') = \delta(\vec{r}-\vec{r}')$$

$$\frac{\delta}{\delta \eta(\vec{r})} \int d\vec{r}' \, \frac{1}{2} \left(\nabla \eta(\vec{r}')\right)^2 = -\nabla^2 \eta(\vec{r})$$

Returning to Model A, we have

$$\frac{\partial \psi(\vec{x},t)}{\partial t} = -\mu \{ -R^2 \nabla^2 \psi(\vec{x},t) + 2\epsilon \psi(\vec{x},t) + 4\psi^3(\vec{x},t) - h \}$$

Model B:

Here we assume $\frac{\partial \psi(\vec{x},t)}{\partial t} = \mu \nabla \cdot J(\psi(\vec{x},t))$

$J(\psi(x,t)) =$ Current

Also $J(\psi(\vec{x},t)) = \nabla \mu(\vec{x},t)$

Thus:

$$\frac{\partial \psi(\vec{x},t)}{\partial t} = \mu \nabla^2 \{ -R^2 \nabla^2 \psi(\vec{x},t) + 2\epsilon \psi(\vec{x},t) + 4\psi^3(\vec{x},t) \}$$

Note that $\nabla^2 h \equiv 0$ since h has been assumed to be spatially constant

Remarks:

1) $\frac{\partial \psi}{\partial t} = \mu \nabla \cdot J$ is a continuity eqn, used for conservation of mass, probability, etc.

2) Models A & B are meanfield

3) Models A & B are nonlinear ⇒ complicated (complex) behavior

4) We are interested in evolution of 2 quantities — $\psi(\vec{x},t)$, and $C(\vec{r})$, where $C(\vec{r}) = \langle \psi(\vec{x},t)\psi(\vec{x}+\vec{r},t)\rangle - \langle\psi(\vec{x},t)\rangle\langle\psi(\vec{x}+\vec{r},t)\rangle$

Here $C(\vec{r})$ is the correlation fn, which can be related to scattering experiments. "$\langle\ \rangle$" refers to ensemble average.

Actually, experiments measure the structure (function) factor, which is the Fourier transform of $C(\vec{r})$:

$$S(\vec{k},t) = \hat{C}(\vec{k},t) = \langle \hat{\psi}(\vec{k},t)\,\hat{\psi}(-\vec{k},t)\rangle$$

Structure Function

Consider a critical quench:

$m = 0$ in Ising model — model B

$h = 0$ in Ising model — model A

We consider an instantaneous quench, and restrict ourselves to linear theory for now.

model A

Crit Quench: $h = 0$ $\underbrace{\epsilon > 0}_{T > T_c} \rightarrow \underbrace{\epsilon < 0}_{T < T_c}$

Initial condition: $\int dx\, \psi(x,t) = 0$ just before & just after quench.

Note: System is unstable, because

$$\Rightarrow \frac{\partial^2 f(\psi)}{\partial \psi^2} < 0 \quad \text{at} \quad \psi = 0 \quad \text{for} \quad \epsilon < 0$$

We investigate evolution away from $\psi = 0$ described by $\psi(\vec{x},t) = u(\vec{x},t)$, and $u(\vec{x},t)$ is assumed to have small amplitude throughout its evolution

Linearizing our kinetic equation –

$$\frac{\partial u(\vec{x},t)}{\partial t} = -M\left\{-R^2\nabla^2 u(\vec{x},t) - 2|\epsilon| u(\vec{x},t)\right\}$$

where $T < T_c$ so $\epsilon < 0$.

Assume $u(\vec{x},t) = \exp(\lambda t)\,\phi(\vec{x})$

Then $\lambda\,\phi(\vec{x}) = M\left\{R^2\nabla^2\phi(\vec{x}) + 2|\epsilon|\,\phi(\vec{x})\right\}$

$$\Rightarrow \quad \lambda = \left(-R^2k^2 + 2|\epsilon|\right)M$$

$$\phi(x) \propto \exp\{i\vec{k}\cdot\vec{x}\} \qquad |\vec{k}| = k$$

General Solution is

$$u(\vec{x},t) = \int c(\vec{k})\, e^{i\vec{k}\cdot\vec{x}} \exp\left[M\left(-R^2k^2 + 2|\epsilon|\right)t\right] d\vec{k}$$

$c(\vec{k})$ are coefficients determined by initial conditions.

<u>However:</u> modes with $R^2k^2 > 2|\epsilon|$ decay
" " $R^2k^2 < 2|\epsilon|$ grow

exponentially with time

This is the type of instability we have been looking for. For $t >> 0$, the $k=0$ mode dominates, although linear theory should not be valid then.

Structure function:

$$\hat{u}(\vec{k},t) = c(\vec{k}) \exp\left[M(-R^2k^2 + 2|\epsilon|)t\right]$$

Linear approximation, critical quench —

$$S(\vec{k},t) \propto \langle \hat{u}(\vec{k},t)\, \hat{u}(-\vec{k},t) \rangle$$

or

$$S(\vec{k},t) \propto \langle c(\vec{k})\, c(-\vec{k}) \rangle \exp\left[2M(-R^2k^2 + 2|\epsilon|)t\right]$$

Since quench is instantaneous, structure factor at $t=0$ is structure factor of the equilibrium state

$$S(\vec{k},0) \sim \langle c(\vec{k})\, c(-\vec{k}) \rangle \sim S_{equil.}(\vec{k})$$

Expression $D(k) = -R^2k^2 + 2|\epsilon|$

Quantity $\exp[D(k)\cdot t]$ is called the amplification factor.

Suppose that $\langle c(\vec{k})\, c(-\vec{k})\rangle = 0$. Then for all $t > 0$, $S(k,t) = 0$, which is nonsense. We must have random fluctuations as part of our system dynamics. We therefore add a noise term $\eta(\vec{x},t)$ to our dynamical equation. This is equivalent to adding a term $\int \eta(\vec{x},t)\, \psi(x,t)\, d\vec{x}$ to the free energy. We assume

typical assumptions

$$\begin{cases} \langle \eta(\vec{x},t)\rangle = 0 \\ \langle \eta(\vec{x},t)\, \eta(\vec{x}+\vec{r},t')\rangle = k_B T\, \delta(\vec{r})\, \delta(t-t') \end{cases}$$

LGW equation with Noise

To obtain $u(\vec{x},t)$ in the limit $\eta(\vec{x},t) \to 0$, we solve

$$\frac{\partial u(\vec{x},t)}{\partial t} = -M\left\{-R^2\nabla^2 u(\vec{x},t) - 2|\epsilon| u(\vec{x},t)\right\} + \eta(\vec{x},t)$$

Linear eqn, so soln is sum of hom. + inhom parts.

To find soln of inhom. part, we first take spatial F.T.:

$$\frac{\partial \hat{u}(\vec{k},t)}{\partial t} = M\left\{-R^2k^2\hat{u}(\vec{k},t) + 2|\epsilon|\hat{u}(\vec{k},t)\right\} + \hat{\eta}(\vec{k},t)$$

Now, solve for Green's fn:

$$\frac{\partial G(t,t')}{\partial t} + M\left\{R^2k^2 - 2|\epsilon|\right\} G(t,t') = \delta(t-t')$$

Let $G(t,t') = G(t-t') = \frac{1}{2\pi}\int \tilde{G}(\omega)\, e^{i\omega(t-t')}\, d\omega$

Then:

$$\tilde{G}(\omega) = \frac{1}{i\omega + M\left\{R^2k^2 - 2|\epsilon|\right\}} = \frac{-i}{\omega - iM\left\{R^2k^2 - 2|\epsilon|\right\}} = \frac{-i}{\omega - \omega_0}$$

We impose the causality condition

KL-31

Evaluate using Cauchy Residue Thm.

$$f(z_0) = \frac{1}{2\pi i}\oint \frac{f(z)}{z-z_0}\,dz \qquad f(z) \text{ analytic}$$

so that for $t > t'$ we close contour in the upper half plane for $R^2k^2 > 2|\epsilon|$, and analytically continue to values of k for which $R^2k^2 < 2|\epsilon|$. Thus:

$$G(t,t') = G(t-t') = \exp\left[-(t-t')\,M\,(R^2k^2 - 2|\epsilon|)\right]$$

Complete soln to dynamical equation $\frac{\partial \hat{u}(\vec{k},t)}{\partial t} = \ldots$ is:

$$\hat{u}(\vec{k},t) = \hat{C}(\vec{k})\exp\left[M(-R^2k^2 + 2|\epsilon|)t\right] + \int_0^t \hat{\eta}(\vec{k},t)\,G(t-t')\,dt'$$

Structure factor:

Is obtained from the product

$$V^{-1}\langle \hat{u}(\vec{k},t')\,\hat{u}(-k,t'')\rangle \qquad \text{where } t = t'-t''$$

↑ Extra factor of V is obtained from an exact treatment of $\langle u(x,t')\,u(\vec{x}+\vec{r},t'')\rangle$ (volume)

see Klein notes 2.42 — Appendix 2A

Then

$$V^{-1}\langle \hat{u}(\vec{k},t')\,\hat{u}(-k,t'')\rangle = V^{-1}\langle \hat{c}(\vec{k})\,\hat{c}(-\vec{k})\rangle \exp[2D(k)t] + V^{-1}\int_0^t\int_0^t \langle \hat{\eta}(\vec{k},t')\hat{\eta}(-\vec{k},t'')\rangle\, G(t-t')\,G(t-t'')\,dt'dt''$$

Note that we have used $\langle \hat{\eta}(\vec{k},t)\rangle = 0$

Also, we use $V^{-1}\langle \hat{\eta}(\vec{k},t')\hat{\eta}(-\vec{k},t'')\rangle = k_B T\,\delta(t'-t'')$

Thus ①

$$(*)\quad S(k,t) = S_0(k)\exp[2D(k)t] + \frac{1}{2D(k)}\left[\exp\{2D(k)t\} - 1\right]$$

② ①

Note: $S_0(k) \equiv V^{-1}\langle \hat{c}(\vec{k})\,\hat{c}(-\vec{k})\rangle$ makes explicit that this is equilibrium structure factor at the pt. where quench is initiated

"Cahn-Hilliard" term ⇒ 1st term tells us about evolution of modes present at time of quench.

"Cook" term ⇒ 2nd term tells us about evolution of terms present as result of fluctuations.

Two final points.

1) Time scale for the evolution is set by $D(k)$, and thus by $|\epsilon|$. If $T \to T_c$, $\epsilon \to 0$, and growth of unstable modes slows down. Since mode at $k=0$ grows fastest, we have characteristic time $\tau \sim \epsilon^{-1} \sim \xi^2$, where ξ is the correlation length. This is called critical slowing down

In general, near crit. pts.,
$\tau \sim \xi^z$ where z is different from 2
Value $z > 2$ is meanfield result for model A.

2) Off-critical quench ($m \neq 0$) is more difficult to describe. Reason is that, in addition to small perturbation, there is large amplitude $k=0$ mode that cannot be treated linearly.

Spinodal Decomposition

Recall that S.D. is the evolution of a system quenched into the unstable region for a conserved order parameter:

Consider: Thus, model B

$$\frac{\partial \psi(\vec{x},t)}{\partial t} = M\nabla^2\left\{-R^2\nabla^2\psi(\vec{x},t) - 2|\epsilon|\psi(\vec{x},t) + 4\psi^3(\vec{x},t)\right\} + \eta(\vec{x},t)$$

Using the condition:

$$\langle \eta(\vec{x},t)\,\eta(\vec{x}',t')\rangle = -k_B T\,\delta(\vec{x}-\vec{x}')\,\delta(t-t')$$

we will derive a result similar to our previous answer for continuous ordering.

First, we linearize:

$$\psi(\vec{x},t) = \psi_0 + w(\vec{x},t)$$

where $w(\vec{x},t)$ is assumed to be small throughout the time period we are studying.

Thus

$$\frac{\partial w(\vec{x},t)}{\partial t} = M\nabla^2\left\{-R^2\nabla^2 w(\vec{x},t) - 2|\epsilon| w(\vec{x},t) + 12\psi_0^2\, w(\vec{x},t)\right\} + \eta(\vec{x},t)$$

In Fourier Space:

$$\frac{\partial \hat{\omega}(\vec{k},t)}{\partial t} = -Mk^2\left\{R^2k^2\hat{\omega}(\vec{k},t) - 2|\epsilon|\hat{\omega}(\vec{k},t) + (2\psi_0^2\hat{\omega}(\vec{k},t)\right\} + \hat{\eta}(\vec{k},t)$$

We obtain

$$\hat{\omega}(\vec{k},t) = \hat{a}(\vec{k})\exp\left[\tilde{D}(k)t\right] + \int_0^t \hat{\eta}(\vec{k},t')\,\tilde{G}(t-t')\,dt'$$

where

$$\tilde{D}(k) = -k^2\left[k^2R^2 - 2|\epsilon| + \psi_0^2\right]$$

(12)

and

$$\tilde{G}(t-t') = \exp\left[(t-t')\,\tilde{D}(k)\right]$$

Structure factor:

$$S(k,t) = \langle \hat{\omega}(k,t)\,\hat{\omega}(-k,t)\rangle$$

$$= S_0(k)\exp\left[2\tilde{D}(k)t\right] + \frac{1}{2\tilde{D}(k)}\left\{\exp\left[2\tilde{D}(k)t\right] - 1\right\}$$

Comparing with previous results on Continuous ordering we see

$$M(-k^2R^2 + 2|\epsilon|) = D(k) \rightarrow \tilde{D}(k) = M(-k^2)\left[k^2R^2 - 2|\epsilon| + \psi_0^2\right]$$

(12)

Also, for C.O., fastest growing mode is at $k=0$:

$$\max\left(-k^2R^2+2|\epsilon|\right) : \frac{\partial}{\partial k}\left(-k^2R^2+2|\epsilon|\right)=0$$

$$\Rightarrow k=0$$

For S.D., fastest growing mode is at nonzero k:

$$\max\left(-k^2\left[k^2R^2-2|\epsilon|+12\phi_0^2\right]\right)$$

$$\rightarrow \frac{\partial}{\partial k}\left(-k^4R^2+2k^2|\epsilon|-12\epsilon^2\phi_0^2\right)=0$$

$$\Rightarrow \boxed{k^2=\frac{|\epsilon|-6\phi_0^2}{R^2}}$$

- Both theories predict, initial growth of structure factor is exponential.

- However, time evolution, which is described by a nonlinear theory, is very different. Also differences in linear regime — interval during which

Linear
$u(\vec{x},t)\ll 1$
$w(\vec{x},t)\ll 1$

linear theory is valid varies with material & system – for some, linear theory is never valid.

Examples:

M Laradji, M Grant, MJ Zuckerman, W Klein, Dynamics of 1st order transitions in d=2 systems with long range interactions, Phys. Rev. B, 41, 4646, 1990.

Examples of Continuous Ordering

(Non-conserved o.p.) $k_c = 0$

Spinodal Decomp

(Conserved o.p.) $k_c \neq 0$

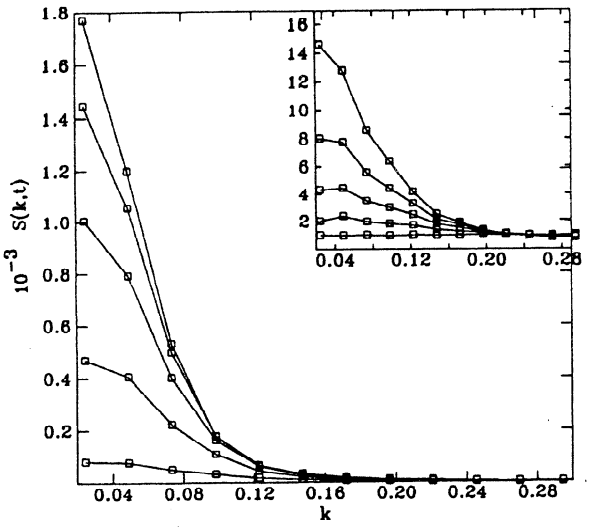

FIG. 2. Structure factor $S(k,t)$ for $R^2=420$. Times are $t=1$, 2, 3, 4, and 5 MCS. Inset shows the very-early-time evolution from 0 up to 0.5 MCS, with a period of 0.125 MCS. (Nonconserved order parameter.)

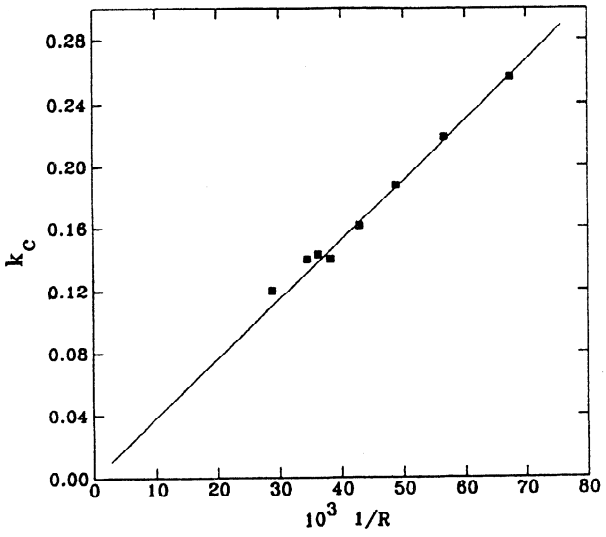

FIG. 4. Critical wave number k_c vs $1/R$. (Nonconserved order parameter.)

the order parameter in phase separation. From observation of coarsening in the configurations, we expect a linear regime (when the fluctuations in the local order parameter are small) for times less than about 60 MCS for $R^2=312$, and about 30 MCS for $R^2=220$. Figure 7 shows the time evolution of the structure factor for $R^2=220$ up to 70 MCS. We note that $S(0,t)$ is fixed during the phase separation due to the conservation law. Note also that the maximum of $S(k,t)$ is approximately fixed for early times. This implies that domains form and become more compact, but their sizes remain approximately constant. As in the order-disorder transition, we fitted the structure factor for $R^2=220$ and 312 to linear theory [Eq. (3)]. The resulting amplification factors are shown in Fig. 8, from which it is evident that,

$$A(k)/k^2 \propto (k_c^2-k^2) ,$$

which is in agreement with Eq. (6) for phase separation. The critical wave number, k_c, was then extracted from the fit in Fig. 8, and the critical wave numbers for both the order-disorder transition and phase separation were

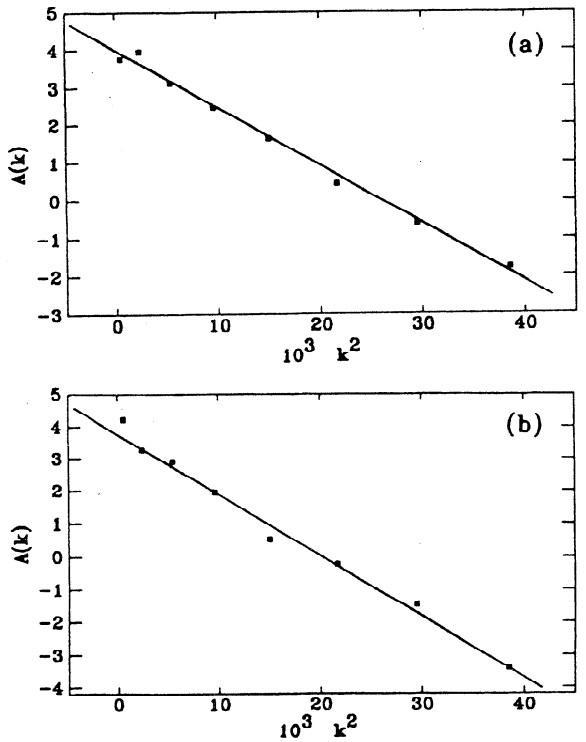

FIG. 3. Amplification factor $A(k)$ vs k^2, for (a) $R^2=544$ and (b) $R^2=760$. (Nonconserved order parameter.)

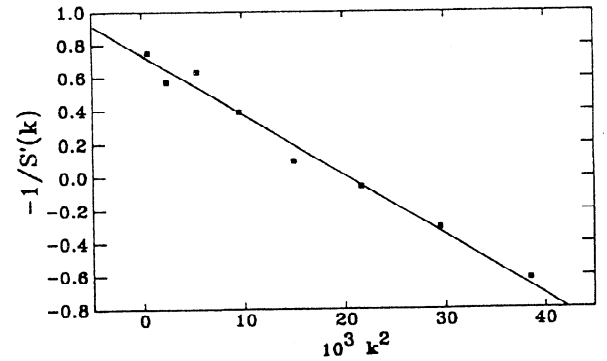

FIG. 5. Fitted results for $-1/S'(k)$ vs k^2 for $R^2=760$. (Nonconserved order parameter.)

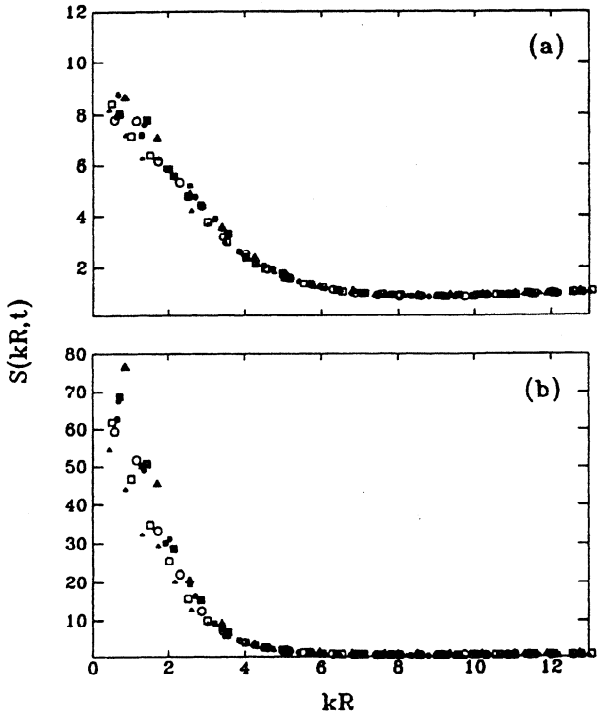

FIG. 6. Scaling of early-time results $S(kR,t)$. Times are (a) $t=0.375$ MCS and (b) $t=0.75$ MCS. (Nonconserved order parameter.)

found to be equal within approximately 12% for $R^2=220$ and 7% for $R^2=312$. This shows that k_c does not depend on the dynamics, but only the local quasiequilibrium aspects of spinodal decomposition. Also, as in the order-disorder transition, we verified the scaling of $S(k,t)$ with R, i.e., $S(kR,t/R^2)$, which is displayed in Fig. 9 for early times.

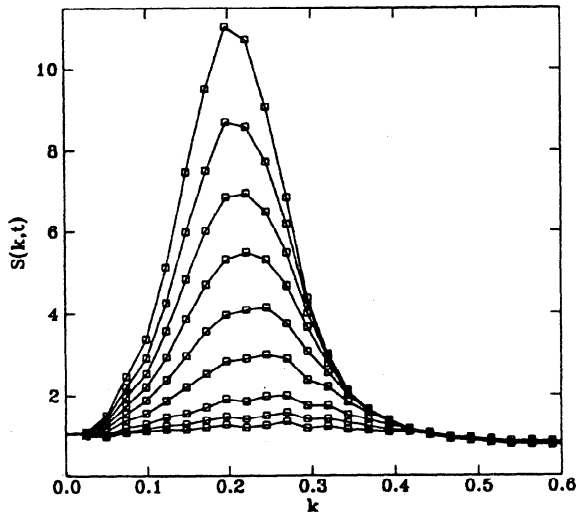

FIG. 7. Structure factor $S(k,t)$ for $R^2=220$. (Conserved order parameter.)

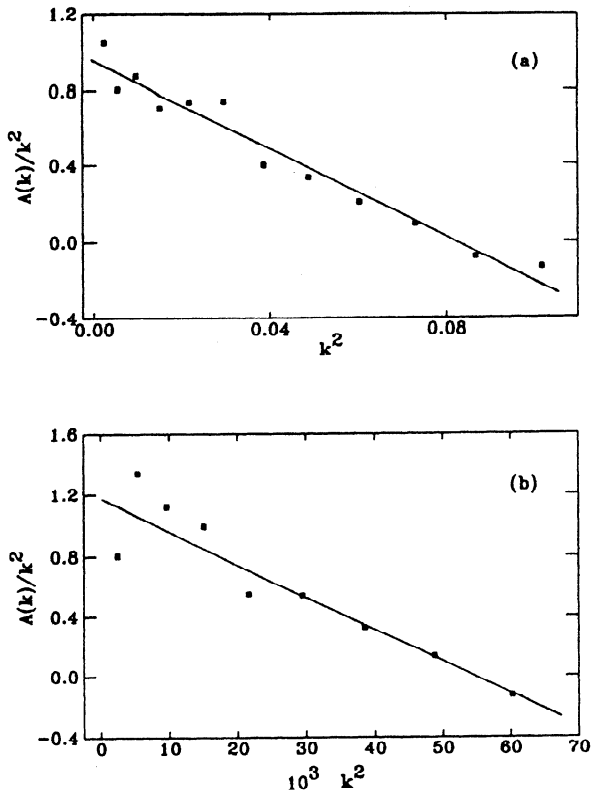

FIG. 8. Amplification factor $A(k)/k^2$ vs k^2, for (a) $R^2=220$ and (b) $R^2=312$. (Conserved order parameter.)

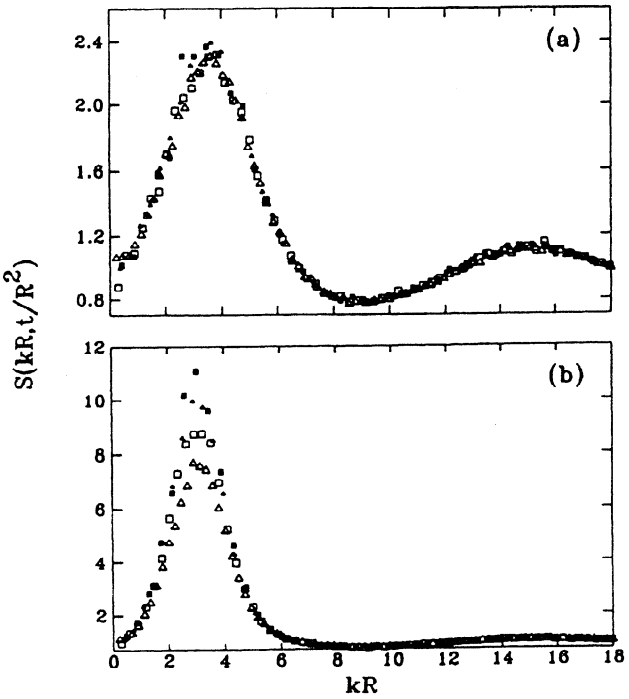

FIG. 9. Scaling of early-time results $S(kR,t/R^2)$. (a) $t/R^2=0.06$ and (b) $t/R^2=0.31$. (Conserved order parameter.)

Classical Nucleation

Problems with this picture of isolated droplets.

1. Real experiments never see critical droplet — droplets only observed after growth has occurred → coalescence

2. Many experiments show nucleation rates that do not scale with h^{-2} as is predicted by classical theory

Previous slide $T = .59 T_c$

Example is shown in next plot:

Metropolis algorithm { Nucleation rate vs $1/h^2$ for Ising model (nearest neighbor) at $.86 T_c$

Another example is shown of nucleation using a different dynamics (Swendsen-Wang algorithm) — clusters

difference is that clusters rather than

KL -21A

J. Stat. Phys 36, 447 (1984)

droplets overcoming the nucleation barrier, and determined from n_s^* for the temperature $T/T_c = 0.59$, is shown in Fig. 6. The straight line is the prediction from Eq. (3.2.1) where the classical prefactor was used and the surface tension was taken to be $=3.1$ (cf. Table 1). For small nucleation rates (small applied field) the data, however, indicate some curvature and are probably not just statistical fluctuations or finite size effects. Kehr and Binder[24] interpreted these deviations as being due to the transition from spherical to cubical droplet shape when the droplet size increases due to a decreasing field.

Deviation from the expected behavior of the nucleation rate was also found for the temperature $T/T_c = 0.86$ (cf. Fig. 7). The nucleation rate shows a curvature and not the expected linear behavior.

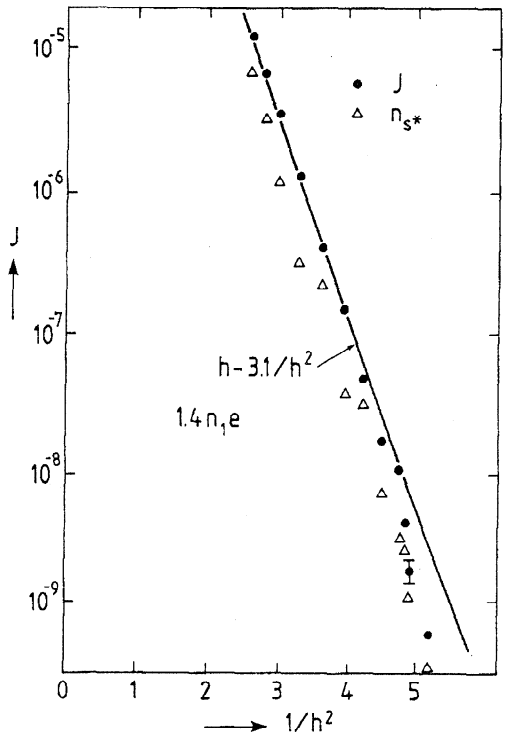

Fig. 6. Nucleation rate plotted logarithmically versus $1/h^2$ for the temperature $T/T_c = 0.59$. The solid line is the prediction from the classical nucleation theory with the surface tension $\sigma/k_B T$ taken from series expansions (Ref. 22). The crosses give the number n_s^* of critical nuclei, as found by our simulations. The dots give the observed nucleation rate.

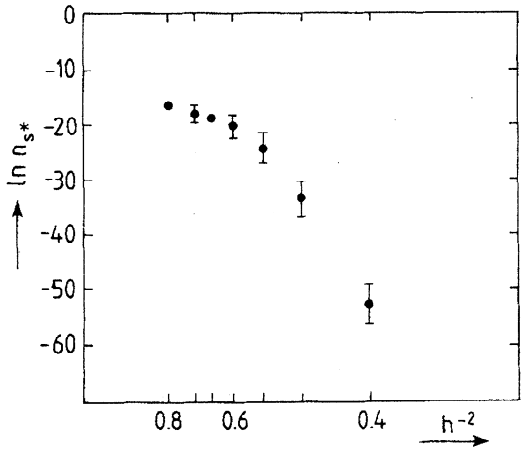

Fig. 7. Nucleation rate as determined by the number of droplets of critical size s^* versus $1/h^2$ for the temperature $T/T_c = 0.86$.

3.3. Growth of Droplets

Finally, let us look at the growth of droplets. According to classical nucleation theory, the growth of droplets after nucleation is governed by the difference of two terms: the incorporation rate and the evaporation rate of monomers, i.e., spins. This approximation should be valid, however, only in the early stages of the growth when the average supersaturation does not change appreciably and for low supersaturations. In the late stages of growth coagulation becomes important due to excluded volume effects.

One takes the incorporation rate and the evaporation rate proportional to the surface area of the droplet, i.e., to $s^{2/3}$. Then the droplet radius, for large s, increases linearly with time. Assuming further that dF_s/ds varies as $s^{-1/3}$ for large s, we obtain

$$(d/dt)s^{1/3} = \text{const}_1 - \text{const}_2\, s^{-1/3} \tag{3.3.1}$$

Figure 8 shows a typical growth process at $T/T_c = 0.59$ and a field $h = 0.45$. After overcoming the nucleation barrier, the droplet grows monotonically and eventually the droplet radius increases linearly with time. In Fig. 8b this growth process is shown for a temperature $T/T_c = 0.86$ and $h = 0.06$. In both cases the modified droplet definition was used. Runs with the Ising definition gave almost the same result.

The above result [Eq. (3.3.1)] was derived under the assumption of a

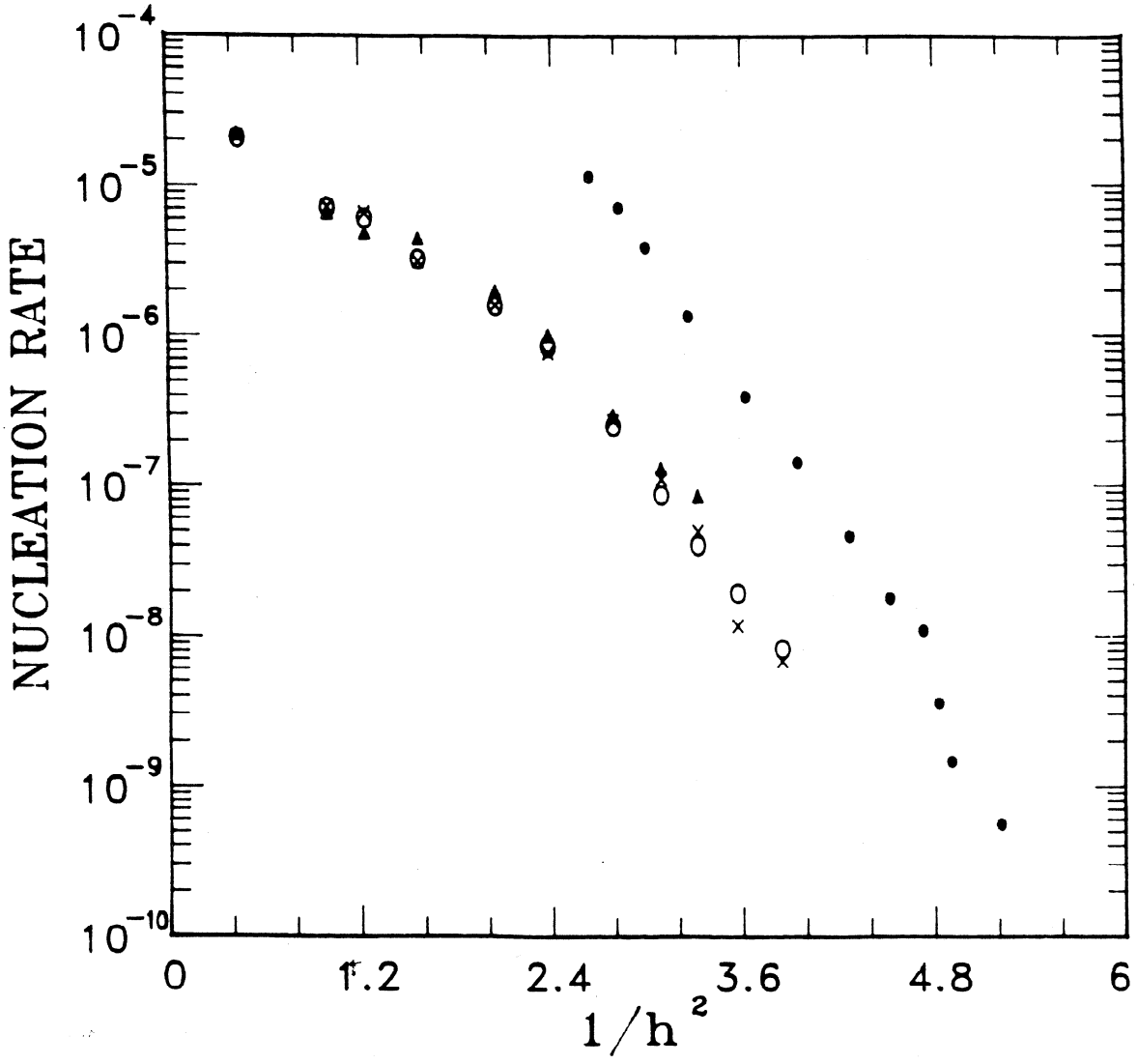

Fig. 3.2 Log of the nucleation rate as a function of h^{-2} for a $d = 3$ Ising model at $0.59T_c$ simulated with the Swendsen-Wang cluster algorithm.

individual spins.

So two simple changes — T & dynamics suffice to produce different results.

Other problems as well — assumptions are made about <u>shape</u> of critical droplet (circular or spherical or hypersphere)

Meanfield descriptions only become precise in limit of long-range interactions when spinodals are precisely defined.

<u>Example</u> Susceptibility $\frac{\partial m}{\partial h}\Big|_T$ as a function of h for various R

Each spin in following plot interacts with q other spins in $d=3$

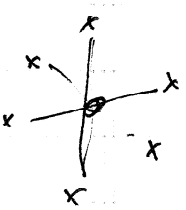

$q=6$ = nearest neighbor
$q=32$ = next nearest neighbor
etc.

Deviation from mean field predictions are observed

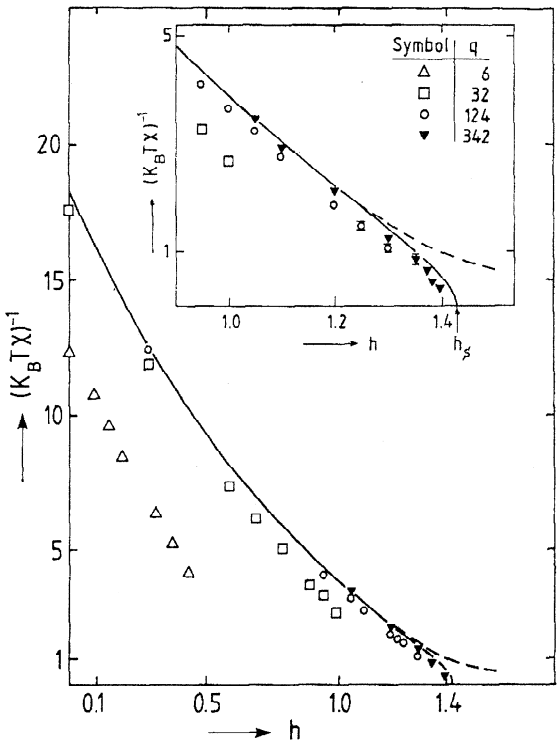

Fig. 10. Inverse susceptibility as a function of the applied field. The full curve is the mean-field prediction for $T/T_c = 4/9$. The spinodal is predicted at $h_s = 1.43$. The broken curve is a fit of the classical nucleation theory to the mean field prediction.

made deeper into the metastable region, which gave almost identical results. Surprisingly, the classical droplet model fits over a wide range. But near the mean-field spinodal, the classical nucleation theory breaks down as can be seen by the Monte Carlo results for $q = 342$. The data follows the mean-field prediction and do not bend over. The figure makes clear that the pseudospinodals converge very rapidly to the mean-field spinodal.

5. A NEW DROPLET MODEL

In Section 3 we used two droplet models, the Ising droplets and the modified droplets (see Definitions 3.1 and 3.2). Here we want to extend the definition of the modified droplets in such a way that the droplets diverge at the mean-field spinodal. The droplets used in nucleation theory of Becker and Döring do not have this property. Their radii stay finite at the spinodal.

(Ref: Vicsek, FGP 2nd ed)

Fractals & Growth

FRACTALS: Term invented by B. Mandelbrot to describe a class of objects that possess similarity properties under change of scale (magnification ↔ shrinkage)

Fractals typically have non-integer dimensions

$$V(l) \sim l^D$$

l - linear dimension
D - fractal dimension

Usually $D < d$ ← Euclidean dimension of embedding space

Applications — dendritic structures, invasion percolation (oil), networks (internet), aggregation of particles, mathematical symmetries, phase transitions, etc.

Prevalence of fractals & scaling in

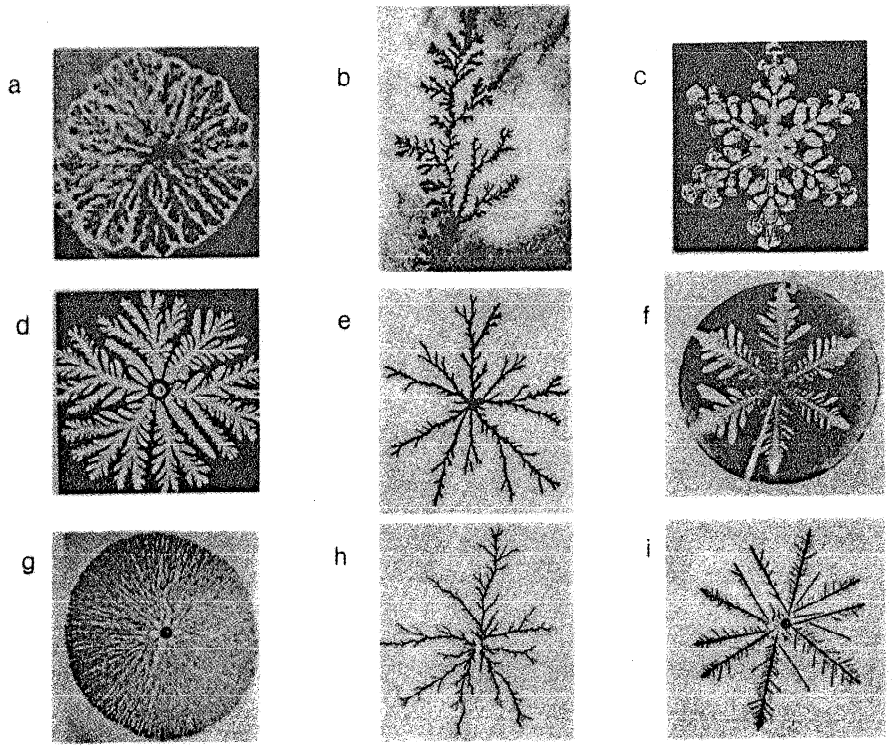

Figure 1. Examples for complex geometrical structures observed in various experiments on growth of unstable interfaces. The three major types of patterns found in the experiments on i) crystallization (a, b and c), ii) viscous fingering (d, e and f), and iii) electrodeposition of zinc (g, h and i) are grouped in separate columns. The fractal dimension of the structures shown in the middle column is close to 1.7. (This set of pictures is reproduced from Vicsek and Kertész (1987). The individual pictures are from: (a) Ben-Jacob et al (1986), (b) Radnóczy et al (1987), (c) Bentley and Humpreys (1962), (d) Buka et al (1986), (e) Daccord et al (1986), (f) Ben-Jacob et al (1985), (g and i) Sawada et al (1986) and (h) Matsushita et al (1984); For details see references to Part III.)

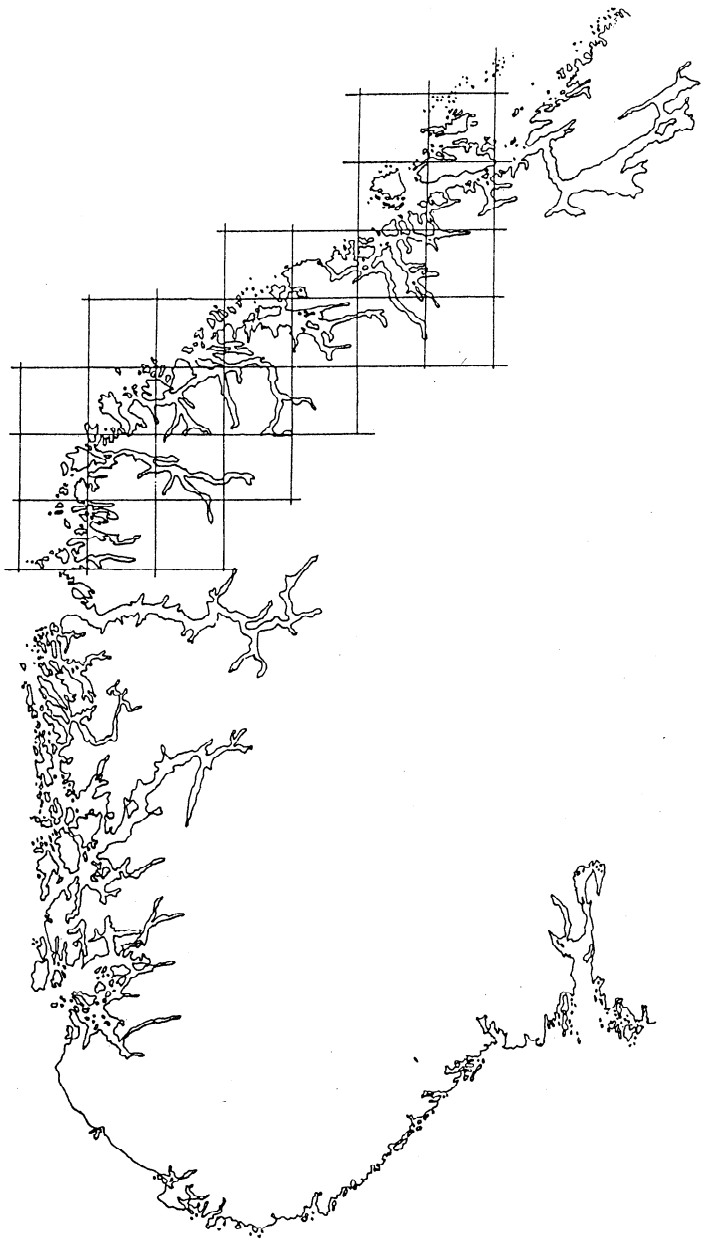

Figure 1 Determining the fractal dimension of the coast of Norway by counting how many boxes the outline of the coast penetrates [Fed 88].

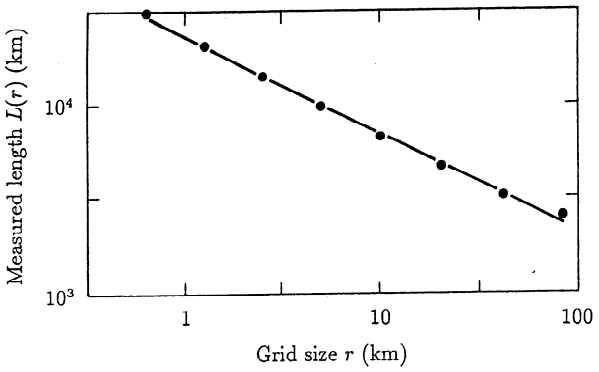

Figure 2 Measured length of Norwegian coast against grid size r. The slope of the straight line gives the fractal dimension of the coast $D \approx 1.52$ [Fed 88].

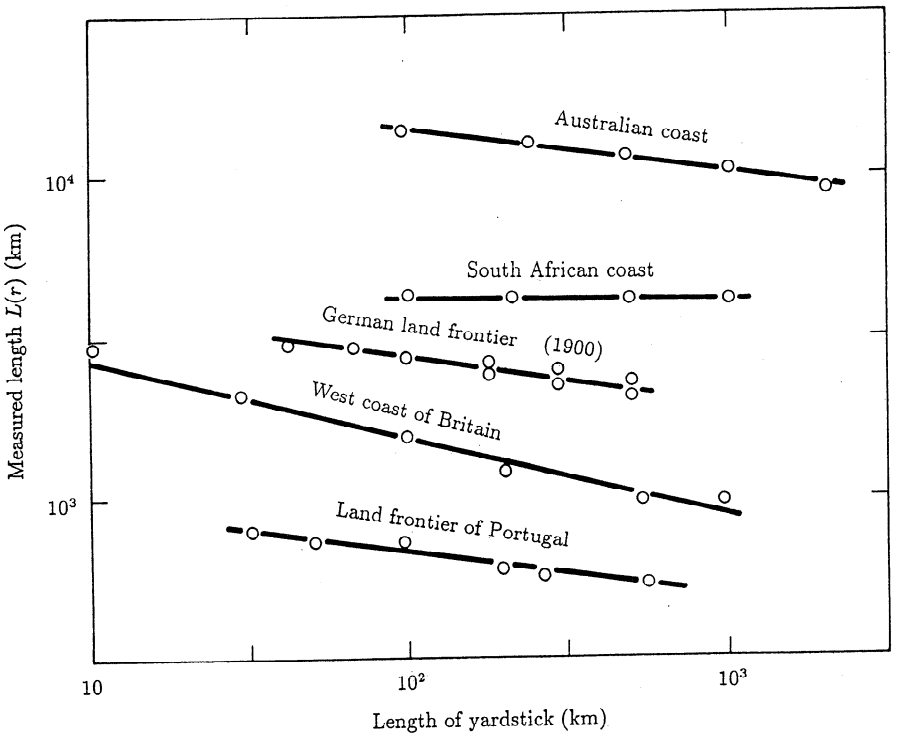

Figure 3 Apparent lengths and fractal dimension of different coasts and land frontiers [Man 83].

phase transitions (droplet structure, symmetries, cluster growth) motivates their study.

Volume of a fractal can be measured by covering it with boxes (or balls) of radius or diameter ℓ.

hypercubic lattice in d dimensions

Then $V(\ell) = N(\ell)\,\ell^d$

"box counting"

where $N(\ell)$ is number of d-dimensional balls needed to cover object completely.

$N(\ell)$ is smallest number of balls for which covering can be achieved.

Examples: Coast of Britain $d=2$; $D \approx 1.3$

etc.

Typically, one finds

$$N(\ell) \sim \ell^{-D}$$

Thus $$D = \lim_{\ell \to 0} \frac{\log N(\ell)}{\log(1/\ell)}$$

In more general notation

Object or system of linear size L

$\epsilon = \frac{l}{L}$, l ~ linear scale of measure

$N(\epsilon) \sim \epsilon^{-D}$, $N(\epsilon)$ is # of d-dimensional balls of radius ϵL needed to cover the fractal.

Types of fractals:

Deterministic – generated by a deterministic rule. e.g.

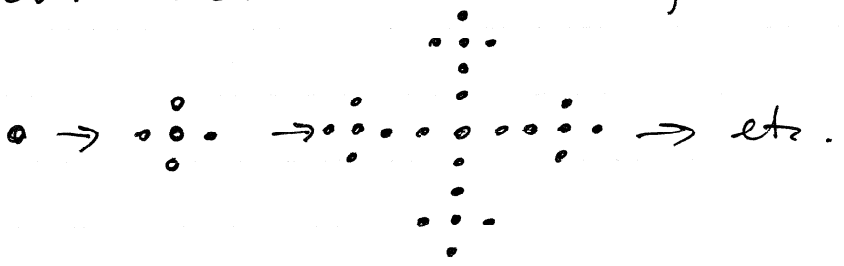

→ etc.

these are "growing fractals"

we shall see that growing droplets are frequently this type of object

Random — Rule has a random component.

Example: Cluster growth, during which a molecule (monomer) is added at random

Random fractals are self-similar only in a statistical sense!

⇒ effective way to describe them is with a pair correlation function

Prob of finding a particle a distance $\vec{r}$ away from another particle

$$C(\vec{r}) = \frac{1}{V} \sum_{\vec{r}'} \rho(\vec{r}+\vec{r}')\,\rho(\vec{r}')$$

Sum is over all sites in the structure

$\rho(\vec{r}) < \begin{matrix} 0 & \text{if vacant site} \\ 1 & \text{if occupied site} \end{matrix}$

$V = N =$ # particles in cluster.

Many fractals are isotropic, so treat

$$C(\vec{r}) = C(r)$$

We can use $C(\vec{r})$ as a criterion for self-similarity

We will define an object to be scale-invariant if $C(r)$ is unchanged up to a constant under rescaling by an arbitrary factor b:

Prob of finding a particle a distance r away from another particle

$$\longrightarrow \quad C(br) \sim b^{-\alpha} C(r)$$

(asymptotically)

α is non-integer, $0 < \alpha < d$

It is easy to show that

$$C(r) \sim r^{-\alpha}$$ (homogeneous function)

We can now compute D from α and d.

Let $N(L)$ be number of particles within a sphere of radius L from origin. Then

$$N(L) \sim \int_0^L C(r)\, d^d r \sim L^{d-\alpha} \sim L^D$$

($C(r)$: prob of finding a particle)

Thus we have the scaling relation

$$D = d - \alpha$$

which can be used to compute D from measurements of density correlations

Example: Cantor middle thirds

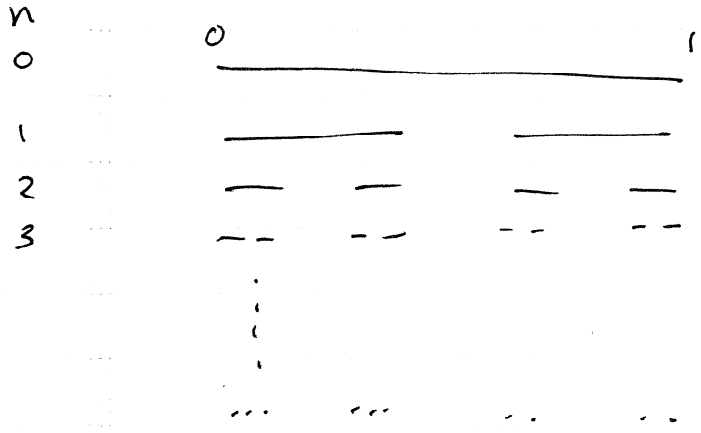

Remove middle 1/3 of line at each generation

$N_n = 2^n$

$l_n = (1/3)^n$

$$D = \frac{\log 2}{\log 3} = \frac{\log N_n}{-\log l_n}$$

$$= .6309$$

Sierpinski:

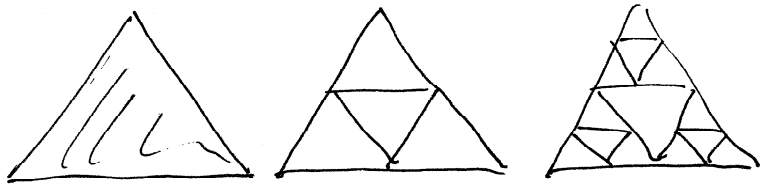

$n = 0$

Remove 1/4 of area at each step

$N_n = 3^n$ $\quad l_n = (1/2)^n$ $\quad D = \frac{\log N_n}{-\log l_n} = \frac{\log 3}{\log 2}$

$= 1.585\ldots$

Other examples:

1. Mandelbrot set, Julia sets:

$$\underbrace{z_{k+1} = z_k^2 - \mu}_{\text{complex \#s}}$$

Test various values of μ in complex plane. Values of μ that yield $z \to \infty$ define M etc.

2. Logistic map

$$x_{n+1} = 4\lambda x_n (1 - x_n)$$

Self-Affine Fractals

$$F(y) \sim b^{-H} F(by), \quad H \text{ some exponent}$$

Example: Brownian motion in $d=1$

$X(t)$ is position:

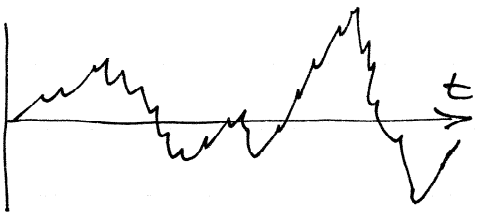

$\langle X_H^2(t) \rangle \sim t^{2H}$ is a special case ($\begin{matrix} b = t \\ y = 1 \end{matrix}$

- H is often called the "Hurst" exponent
- When $0 < H \neq 1/2 < 1$, the random walk is called a "fractional Brownian motion", or "fBm"
- When jumps are independent, and distance increments have a Gaussian distribution, $H = 1/2$
- Note: $D_B = 2 - H$, where D_B is box-counting dimension

Proof: During a time interval δt,

$$|\max[X_H(t)] - \min[X_H(t)]| \sim \delta t^H$$

Covering the piece of $X_H(t)$ on the interval δt by squares of side length δt requires $\sim \frac{(\delta t)^H}{\delta t} = \delta t^{H-1}$ squares

Therefore $N(\delta t) \cdot \delta t \tilde{=} (\delta t)^{H-1}$

or $N(\delta t) \sim (\delta t)^{H-2}$

Since $N(\delta t) \sim \frac{1}{(\delta t)^D}$, we have

$$D = 2 - H$$

- Note also that if the Fourier transform of $X_H(t)$ is $\hat{X}_H(f)$, then

$$|\hat{X}_H(f)| \sim f^{-H-1/2}$$

Alternatively, the power spectrum scales as $|\hat{X}_A(f)\,\hat{X}_H(-f)| \sim f^{-\beta}$

and we find $\beta = 2H+1$.

Proof is left to the student.

Multifractals:

Time-independent distributions defined on a

fractal substrate are called "fractal measures."

More generally, a fractal measure has an infinite number of singularities — expressed by term "multifractal"

Example: Deterministic recursive (multiplicative) process — generates a non-spatially uniform fractal with varying weights or probabilities attributed to each re-scaled part.

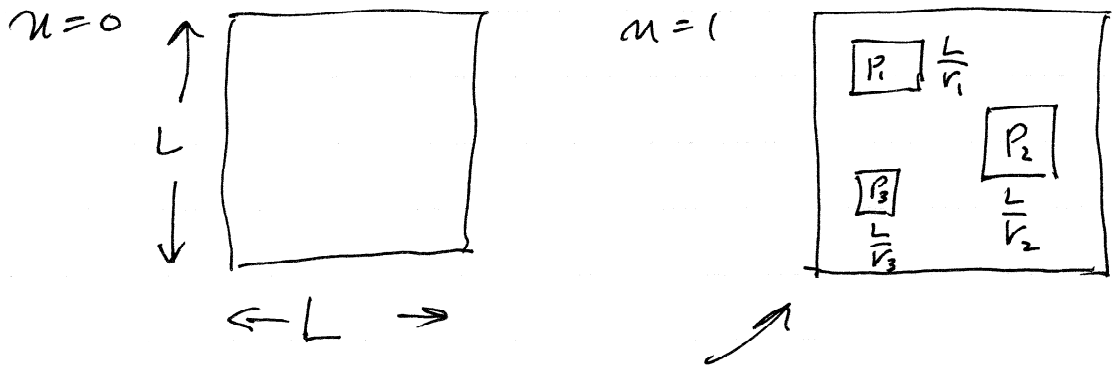

reduction factors $\frac{L}{r_i}$; weight P_i ← Replace original square by 3 smaller copies

Steps:

1. Replace original square (weight = P = 1) having side length (scale) L by 3 smaller squares — weights P_i, side lengths $\frac{L}{r_i}$ $r_i > 1$.

2. Repeat #1 in each smaller square so that we now have $3^2 = 9$ smaller squares.

Number of smaller squares $= 3^n$

Weights of smaller squares is a product: $P_i P_j \cdots P_n$

Side lengths of smaller squares is a product $\frac{L^n}{r_i \cdot r_j \cdots r_n}$

$\Longrightarrow$ a square that goes thru a $\frac{1}{r_i}$ reduction each time has a

side length $\frac{L^n}{r_i^n}$ and a weight p_i^n.

Probability Measures of Multifractals

- We cover the fractal with a d-dimensional hypercubic lattice

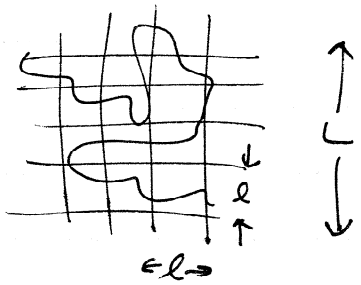

- Denote by p_i the probability (or "mass") associated with i^{th} box

$$p_i = \int_{i^{th}\ box} d\mu(\vec{x}) \quad , \quad \sum_i p_i = 1$$

How does p_i vary with box size?

- Let $\epsilon \equiv \frac{\ell}{L}$, want $\epsilon \to 0$

- For homogeneous structure (uniform mass density) $p_i(\epsilon) \sim \epsilon^d$

- For a uniform fractal ($r_i \equiv r$) of

dimension D :

Define — Volume of Support

$\Rightarrow$ volume of i^{th} d-dimensional box with mass

Thus, $p_i(\epsilon) \sim \epsilon^D$, $D < d$, since for a uniform density, p_i is the volume of support for i^{th} box.

Note: Density of i^{th} box is then

$$\rho \sim \frac{\epsilon^D}{\epsilon^d} = \epsilon^{D-d}$$

- For a non-uniform fractal, we are led to assume a general form

$$p(\epsilon) \sim \epsilon^\alpha \quad , \quad \epsilon << 1$$

α can take on a range of values depending on the given box used.

- Exponent α corresponds to the strength of the local singularity of the measure — sometimes called the "crowding index" or "Hölder" exponent.

- α depends on which box is used, i.e., $\alpha = \alpha(\vec{x}_i)$, where $\vec{x}_i$ locates center of the d-dimensional hyper-cubic box.

$\Rightarrow$ There are usually many boxes with the same index α.

The number of such d-dimensional boxes having exponent α is assumed to scale as

$$N_\alpha(\epsilon) \sim \epsilon^{-f(\alpha)}$$

So $f(\alpha)$ is the "fractal dimension" of the subset of boxes having

exponent α.

- Exponent α can take on values on an interval $[\alpha_\infty, \alpha_{-\infty}]$ —

$f(\alpha)$ is usually a single, humped function with a maximum

$$\max_{\alpha} f(\alpha) = D$$

- The $f(\alpha)$ spectrum of an ordinary (mono-) fractal is a single point on the $f-\alpha$ curve.

- Typical fractal is assumed to be made of an interwoven set of singularities of strength α, each characterized by its own fractal dimension $f(\alpha)$.

Computation of Exponents

An important quantity is:

$$\chi_q \equiv \sum_i p_i^q \quad , \quad -\infty < q < \infty$$

(Similar to Rényi entropy)

For $q=0$, χ_q gives # of boxes needed to cover the fractal support (the region where mass is), $N(\epsilon)$
$p_i \neq 0$

Thus $\chi_0 = N(\epsilon) \sim \epsilon^{-D}$

Since distribution is normalized, i.e., $\sum_i p_i = 1$, we have

$$\chi_1 = \sum_i p_i = 1$$

Due to complexity of multifractal distributions, scaling of χ_q for $\epsilon \to 0$ depends on q non-trivially:

$$\chi_q \sim \epsilon^{(q-1) D_q}$$

where D_q is the "order q generalized dimension"

- We will find that D_q's are not fractal dimensions

For all q, we have D_q o $\Leftrightarrow$ note that $\chi_1 = 1$ satisfied automatically

- Can be shown that D_q's decrease monotonically for increasing q.
- $D_0 = D$
- Uniform fractals, $D_q = D$, all q.
- As $\epsilon \to 0$, dominant contribution to $\chi_q = \sum_i p_i^q$ comes from a subset of all boxes — this

subset is a fractal with dimension

f_q — $N_q \sim \epsilon^{-f_q}$

# of boxes giving essential contribution to χ_q; all of these boxes have $p_i = p_q$

- Denote $p_q \sim \epsilon^{\alpha_q}$, $\epsilon \to 0$

  So f_q and α_q provide an alternative description to $p(\epsilon) \sim \epsilon^{\alpha}$; $N_\alpha(\epsilon) \sim \epsilon^{-f(\alpha)}$

- Primary contribution to $\chi_q(\epsilon)$ comes from boxes where $N(\alpha,\epsilon) p_i^q$ is maximal, where $N(\alpha,\epsilon)$ is number of boxes with α.

- Using $\chi_q(\epsilon) \sim N_q(\epsilon) p_i^q \sim \epsilon^{(q-1)D_q}$

  $\sim N_q(\epsilon) p_q^q$

  and $N_q(\epsilon) \sim \epsilon^{-f_q}$; $p_q \sim \epsilon^{\alpha_q}$

e.g.

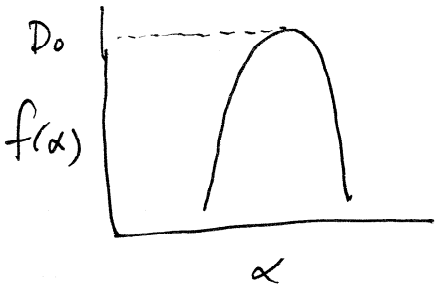

we obtain

$$(q-1)\,D_q = q\,\alpha_q - f_q$$

- Using $p(\epsilon) \sim \epsilon^{\alpha}$; $N_\alpha(\epsilon) \sim \epsilon^{-f(\alpha)}$;

and $\chi_q(\epsilon) = \sum_i p_i^q$, $\epsilon \to 0$

we pass to a continuum limit and write

$$\chi_q(\epsilon) \sim \int_{a_{-\infty}}^{a_\infty} \epsilon^{q\alpha' - f(\alpha')}\, d\alpha'$$

For $\epsilon \ll 1$, integral dominated by value of α that minimizes the exponent.

$\frac{d}{d\alpha}(q\alpha - f(\alpha)) = 0$

Thus $$\left.\frac{df(\alpha)}{d\alpha}\right|_{\alpha_q} = q$$

α_q is value for which $q\alpha - f(\alpha)$ is minimized.

- Also, $f_q = f(\alpha_q)$ (obviously)

Models of Fractal Growth

We will examine a number of models for growing clusters. We will need to determine fractal dimensions.

Typically, we choose a scale ℓ, $\epsilon = \ell/L$, and cover the fractal with a d-dimensional hypercube, where d is the lowest dimension we can use.

Then we compute $N \sim$ number of ℓ-boxes that have mass in them.

So we determine $N \sim \epsilon^{-D}$

Plot

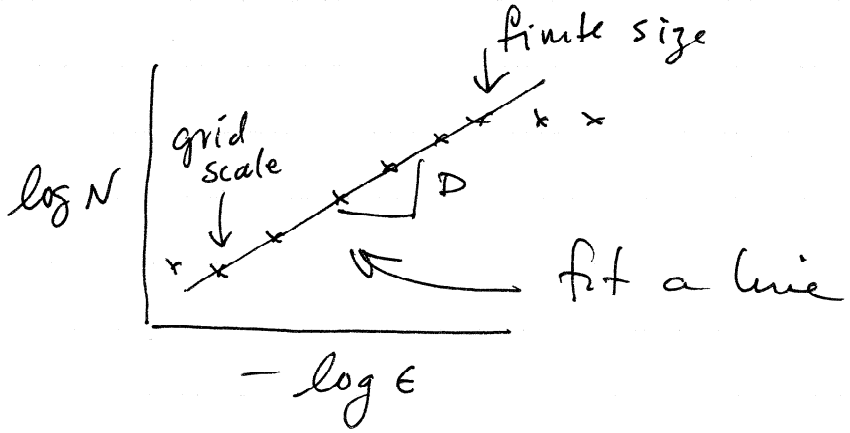

There are complications at large & small ϵ

Clusters - Structures of particles or occupied sites that can be connected by bonds (often, nearest-neighbor) are called clusters or aggregates.

I Site percolation

- Lattice - occupy sites with prob p_{occ}
- Go thru lattice sites "typewriter fashion" test each site with random number generated from uniform dist^n on $[0,1]$.
- If $p_{ran} < p_{occ}$, occupy the site. If $p_{ran} > p_{occ}$, move on to next site.
- Count clusters

II Forest fire Model

- Pick a site a random. If it is vacant, occupy it with a "tree".
- At same time, drop "matches" or "lightning bolts" with frequency f_{spark}

(i.e., once every, say 1000 tree planting time steps). If spark hits a tree in a cluster, burn all trees in cluster and declare the sites vacant.

- Continue with this program & record clusters that are burned.

III Spreading Percolation

- Lattice as usual. Begin with 1 site as the initial seed (occupied)
  - Neighbor sites considered to be "live sites"
  - A live site is chosen at random and (i) occupied with prob. p, or (ii) killed for all time with prob. $1-p$
  - Filled site becomes part of growing cluster and its new neighbors are now live sites

- Continue until all sites become occupied or killed

⇒ this model applies to epidemics, chemical reactions, flame propagation

IV Invasion Percolation

- Simulates displacement of one fluid by another in a porous medium under condition that capillary forces dominate

Ex: Oil displaced by water in an oil reservoir at slow rate

→ 1) a random # drawn from uniform distribution on [0,1] is assigned to each site

2) Like spreading percolation, process begins w/ seed particle and continues by occupation of (empty) perimeter sites